Contents

The following Communications have been judged by at least two referees to be "very important papers" and will be published online at www.angewandte.org soon:

M. Mascal, E. B. Nikitin*
Direct, High-Yield Conversion of Cellulose into Biofuel

P. García-Álvarez, D. V. Graham, E. Hevia, A. R. Kennedy, J. Klett, R. E. Mulvey, C. T. O Hara, S. Weatherstone*
Unmasking Representative Structures of TMP-Active Hauser and Turbo Hauser Bases

*T. Robert, J. Velder, H.-G. Schmalz**
Enantioselective Copper-Catalyzed 1,4-Addition of Grignard Reagents to Cyclohexenone Using Taddol-Derived Phosphine–Phosphite Ligands and 2-Methyl-THF as a Solvent

*A. D. Shaller, W. Wang, H. Gan, A. D. Q. Li**
Tunable Molecular Assembly Codes Direct Reaction Pathways

D. Staack, A. Fridman, A. Gutsol, Y. Gogotsi, G. Friedman**
Nanoscale Corona Discharge in Liquids Enabling Nanosecond Optical Emission Spectroscopy

*C. Hawner, K. Li, V. Cirriez, A. Alexakis**
Copper-Catalyzed Asymmetric Conjugate Addition of Aryl Aluminum Reagents to Trisubstituted Enones: Construction of Aryl-Substituted Quaternary Centers

*K. W. Eberhardt, C. L. Degen, A. Hunkeler, B. H. Meier**
One- and Two-Dimensional NMR Spectroscopy with a Magnetic-Resonance Force Microscope

*S. Wan, J. Guo, J. Kim, H. Ihee, D. Jiang**
A Belt-Shaped, Blue-Luminescent and Semiconducting Covalent Organic Framework

News

Books

Appeal

Computational Studies

To be or not to be: The terms "viable" and "fleeting," rather than the imprecise term "stable," are proposed to describe hypothetical molecules whose existence has been predicted by computational studies. A number of criteria that a molecule described as viable should fulfill are discussed.

Referee Report

Computational Studies

Contents

Essays

Peer Review

Refereeing the referees: The peer review process of *Angewandte Chemie* has been examined according to the criteria of reliability (agreement between referees) and predictive validity (correlation between publication decision and citation frequency of the reviewed work). Despite the dramatic increase in submitted manuscripts and significant decline in acceptance rate, the results show the unwavering quality of the peer review at *Angewandte Chemie*.

Reviews

Natural Products

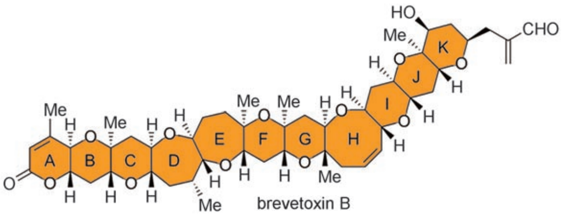

Natural products with cyclic ethers: The discovery of brevetoxin B in 1981 marked the beginning of the marine polyether biotoxins saga that still fascinates chemists and biologists. This Review gives a chronological overview of the developments in this research field, including studies on the isolation, chemical synthesis, and chemical biology of these toxins.

Communications

Chiral Resolution

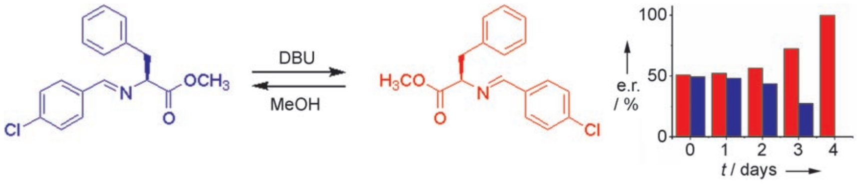

Just bead it! Despite the complication of enantiomeric epitaxial behavior, a derivative of phenylalanine was completely resolved (see picture). Racemization takes place by abrasively grinding crystals of the compound in a saturated solution. By studying the influence of different crystal sizes, it was found that Ostwald ripening plays an important role in this process. DBU = 1,8-diazabicyclo-[5.4.0]undec-7-ene.

For the USA and Canada: ANGEWANDTE CHEMIE International Edition (ISSN 1433-7851) is published weekly by Wiley-VCH, PO Box 191161, 69451 Weinheim, Germany. Air freight and mailing in the USA by Publications Expediting Inc., 200 Meacham Ave., Elmont, NY 11003. Periodicals postage paid at Jamaica, NY 11431. US POSTMASTER: send address changes to *Angewandte Chemie*, Wiley-VCH, 111 River Street, Hoboken, NJ 07030. Annual subscription price for institutions: US$ 7225/6568 (valid for print and electronic / print or electronic delivery); for individuals who are personal members of a national chemical society prices are available on request. Postage and handling charges included. All prices are subject to local VAT/ sales tax.

Heterocycles

S. Würtz, S. Rakshit, J. J. Neumann,
T. Dröge, F. Glorius* ——— 7230 – 7233

Palladium-Catalyzed Oxidative Cyclization of *N*-Aryl Enamines: From Anilines to Indoles

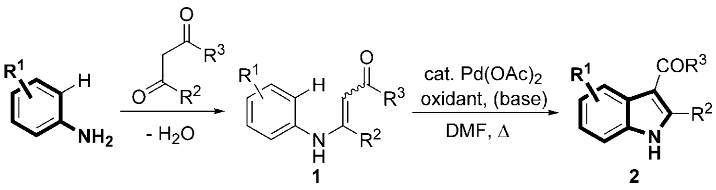

The special advantage of the title reaction to form substituted indoles **2** lies within the broad scope of the transformation: A multitude of *N*-aryl enaminones **1** can be prepared readily in one step from commercially available anilines. Furthermore, anilines can be converted directly in a one-pot process into the indole products. $R^1 = H$, Me, OMe, Cl, F, carbonyl functionality, CN, fused aryl; $R^2 =$ alkyl, aryl; $R^3 =$ alkyl, O–alkyl.

Cluster Compounds

G. Prabusankar, A. Kempter, C. Gemel,
M.-K. Schröter,
R. A. Fischer* ——— 7234 – 7237

$[Sn_{17}\{GaCl(ddp)\}_4]$: A High-Nuclearity Metalloid Tin Cluster Trapped by Electrophilic Gallium Ligands

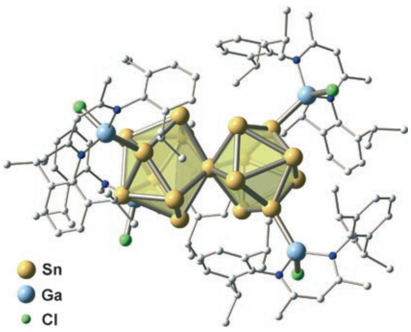

The reduction of $SnCl_2$ by the low-valent gallium(I) β-diketiminate Ga^{I}(ddp) gives the title complex, which is best described as a Zintl-type anionic $[Sn_{17}]^{4-}$ cluster stabilized by an electrophilic shell of gallium ligands. This reaction could represent a new concept for the synthesis of metalloid main-group clusters. ddp $= HC(CMeNC_6H_3\text{-}2,6\text{-}iPr_2)_2$.

Surface Chemistry

T. Winkler, N. Ballav, H. Thomas,
M. Zharnikov,* A. Terfort* — 7238 – 7241

Micrometer-Scale Protein-Resistance Gradients by Electron-Beam Lithography

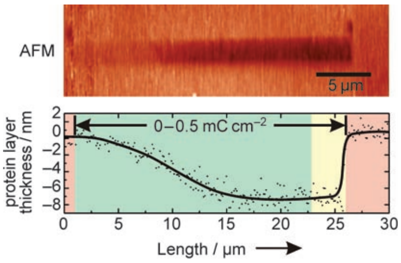

Sticky slope: The irradiation-promoted exchange reaction on monolayers using ethylene glycol terminated thiols as ligands provides a useful tool for the adjustment of the bioresistance of surfaces. In conjunction with electron-beam lithography, micrometer-scale gradients of protein adhesivity could be produced (see picture: AFM = atomic force microscopy).

Peptidyltransferases

M. Koch, Y. Huang,
M. Sprinzl* ——— 7242 – 7245

Peptide-Bond Synthesis on the Ribosome: No Free Vicinal Hydroxy Group Required on the Terminal Ribose Residue of Peptidyl-tRNA

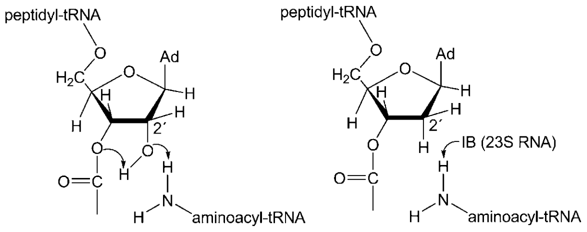

OH?—OH no! The generally accepted explanation for peptide transfer in ribosomal peptidyltransferase is that the 2′-OH group of the adenosine residue (Ad) in the P site accepts a proton from the incoming α-amino group and transfers it to the outgoing deacylated tRNA (left). However, it has now been shown that peptide transfer still takes place in the absence of the 2′-hydroxy group (right: proposed alternative mechanism).

Metal–Metal Bonds

Shorter than ever: Reduction of chromium(II/III) chlorides stabilized by amidopyridinato ligands leads to a dichromium complex that has a Cr–Cr bond length of 1.75 Å. This bond is exceptionally short, even for bonding orders higher than four, and is at present the shortest reported metal–metal bond for a stable compound. The experimental results are supported by theoretical calculations.

Quintuple Bonds

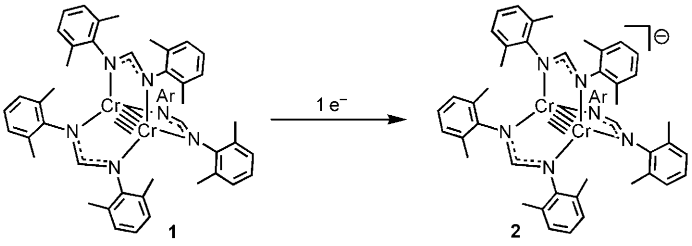

The shortest metal–metal bond so far is found in complex anion **2** (Cr–Cr 1.7397(9) Å), which is the one-electron reduction product of thermally stable mixed-valent complex **1** (see scheme). Experimental data unambiguously show that the electronic configuration of **1** is $\sigma^2\pi^4\delta^3$, and theoretical studies confirm the presence of a Cr–Cr quintuple bond in **2**. Ar = $2,6\text{-}C_6H_3(CH_3)_2$.

Mesoporous Sensors

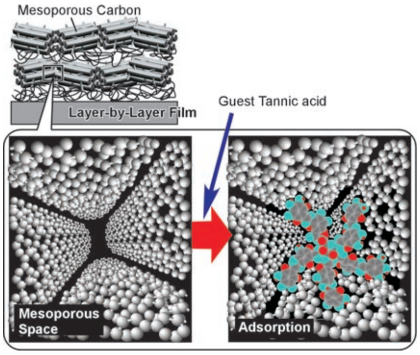

Tea or coffee? The layer-by-layer assembly of mesoporous carbon onto a quartz crystal microbalance results in a structure (see picture) that can be used for highly selective in situ measurement of nonionic aqueous guests, such as tea components.

DNA Detection

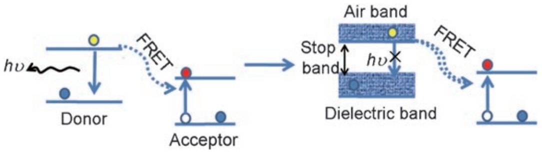

A strong signal: A fluorescence resonance energy transfer (FRET)-based DNA hybridization detection method uses a photonic crystal to amplify the optical signal (see picture). Single-mismatch selectivity and a sensitivity of about 13.5 fM are achieved.

Open and close: Inspired by close-packing of spheres, to strengthen the framework–H_2 interaction in MOFs (metal-organic frameworks), a strategy is devised to increase the number of nearest neighboring open metal sites of each H_2-hosting cage, and to align the open metal sites toward the H_2 molecules. Two MOF polymorphs were made, one exhibiting a record high hydrogen uptake of 3.0 wt% at 1 bar and 77 K.

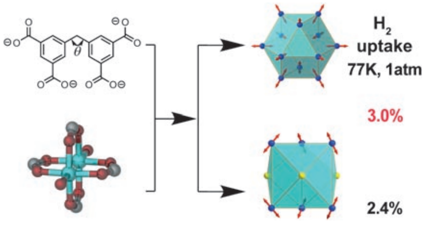

A number of human pathologies have been linked to the conversion of soluble proteins into amyloid aggregates. A new computational method based on first principles, peptide interaction matrix analyzer, identifies aggregation-prone peptides, which form in-register antiparallel (see picture) or parallel β sheets, and predicts the likelihood of coaggregation within or between proteins.

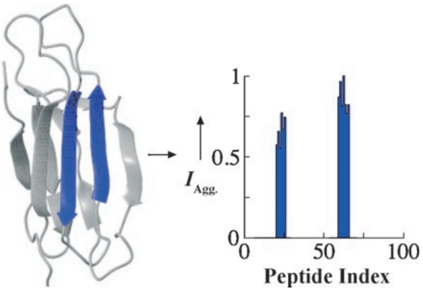

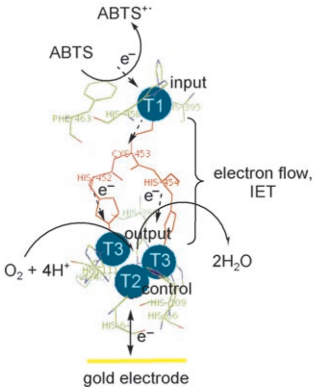

Potential for change: The activity of a fungal laccase on a gold electrode can be modulated by an applied potential. The activity–potential dependence resembles “transistor-like” current–potential characteristics. The applied potential affects the chemical and electronic structure of the T2/T3 copper cluster of the enzyme by a mechanism similar to that of the natural regulation of laccase activity (see scheme; IET: intramolecular electron transfer).

Twisted fibers with a helical structure are formed by self-assembly of chiral polyoxomolybdates (POMs) $[(R^*PO_3)_2Mo_5O_{15}]^{2-}$ (R = $CH_3CH(NH_3)$, $CH_3CH(CH_3)CH(NH_3)$) through H-bonding. High-resolution TEM images of single fibers show an ordered substructure with parallel rows about 2 nm in width, in agreement with the packing of the H-bonded POM subunits in the X-ray structure (see inset).

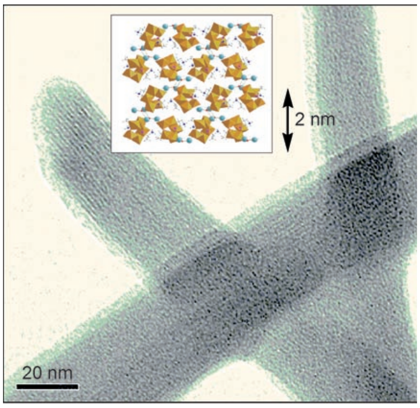

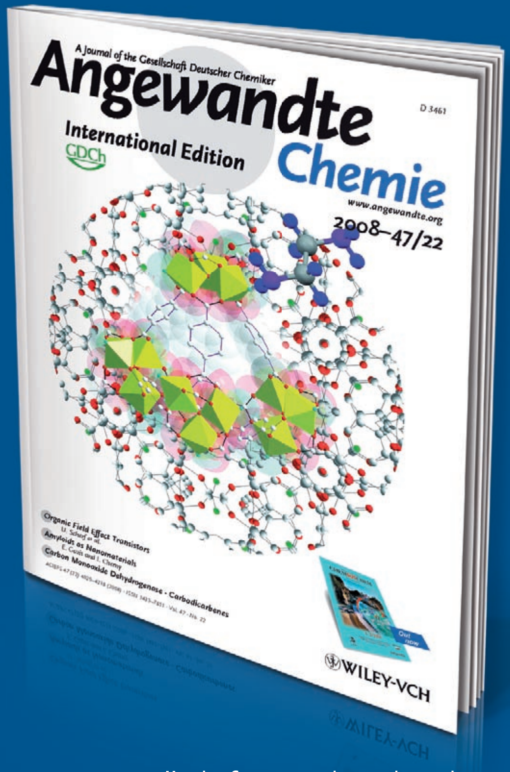
A Journal of the Gesellschaft Deutscher Chemiker
Angewandte
International Edition
GDCh
Chemie
D 3461
www.angewandte.org
2008–47/22
WILEY-VCH

Ligand Design

A. Q. Hassan, J. T. Koh* ___ 7280–7283

Selective Chemical Rescue of a Thyroid-Hormone-Receptor Mutant, TRβ(H435Y), Identified in Pituitary Carcinoma and Resistance to Thyroid Hormone

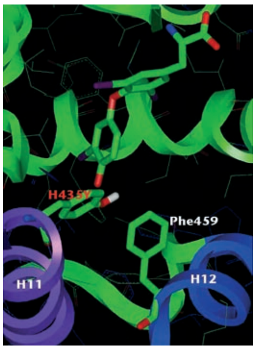

Ligand to the rescue! Thyroid hormone receptor (TR) plays a critical role in development and homeostasis. The mutant TRβ(H435Y) was identified in both cancer and resistance to thyroid hormone. A designed synthetic ligand recovered the cellular reporter-gene activity of TRβ(H435Y) with a 5850-fold improvement in selectivity for the mutant relative to that of the natural hormone T3 (shown in a modeled structure with TRβ(H435Y)).

Biological Imaging

J.-H. Park, G. von Maltzahn, E. Ruoslahti, S. N. Bhatia, M. J. Sailor* ___ 7284–7288

Micellar Hybrid Nanoparticles for Simultaneous Magnetofluorescent Imaging and Drug Delivery

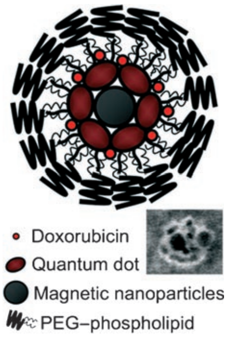

Multimodal nanoassemblies that contain magnetic nanoparticles, quantum dots, and the anticancer drug doxorubicin within a single PEG–phospholipid micelle were prepared (see scheme; PEG = poly(ethylene glycol)). When equipped with the targeting peptide F3, these nanostructures enable simultaneous targeted drug delivery and dual-mode imaging of tumor tissues by near-infrared fluorescence and NMR spectroscopy.

Protein Detection

Y. Nakamura, R. Miyatake, M. Ueda* ___ 7289–7292

Enantiodifferential Approach for the Detection of the Target Membrane Protein of the Jasmonate Glycoside that Controls the Leaf Movement of *Albizzia saman*

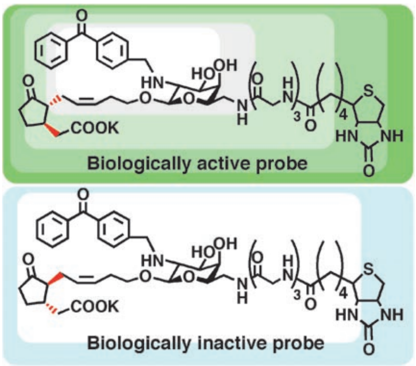

Pairs of probes with recognition elements of opposite configuration can be used to detect target proteins of biologically active natural products. The diastereomeric probes shown were designed on the basis of structure–activity relationships determined for an endogenous factor that controls leaf opening and closing in the title plant. They revealed that a 38 kDa membrane protein is key to the stereospecific recognition of the natural product.

Supramolecular Chemistry

Y. Liu,* J. Shi, Y. Chen, C.-F. Ke ___ 7293–7296

A Polymeric Pseudorotaxane Constructed from Cucurbituril and Aniline, and Stabilization of Its Radical Cation

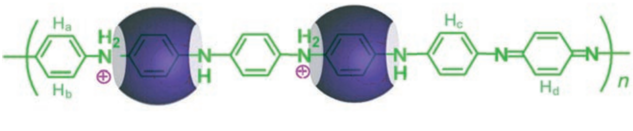

1

Picking up the thread: A polypseudorotaxane **1** with a regular one-dimensional linear structure has been constructed in satisfactory yield from cucurbit[7]uril and polyaniline (PANI). The complexation with cucurbituril not only enhances the water solubility of the PANI (see picture; after 10 h), but also effectively stabilizes its radical cation form, that is, the conductive doped form, as shown by EPR spectroscopy.

Contents

Membrane Proteins

A. Gautier, J. P. Kirkpatrick,
D. Nietlispach* ______ **7297 – 7300**

Solution-State NMR Spectroscopy of a Seven-Helix Transmembrane Protein Receptor: Backbone Assignment, Secondary Structure, and Dynamics

Protein in motion: A solution-state NMR study on the seven-helix transmembrane protein pSRII (see picture) in a detergent solution focused on the sequential backbone assignment, the characterization of the secondary structure, and the backbone dynamics. The structural integrity of the protein was confirmed, and mobility in the loops (ps–ns timescale) and slower motions in the helical core (µs–ms timescale) were identified.

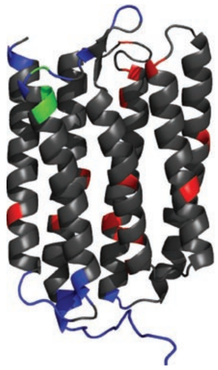

Nanostructures

Y. S. Zhao, J. Xu, A. Peng, H. Fu, Y. Ma,
L. Jiang, J. Yao* ______ **7301 – 7305**

Optical Waveguide Based on Crystalline Organic Microtubes and Microrods

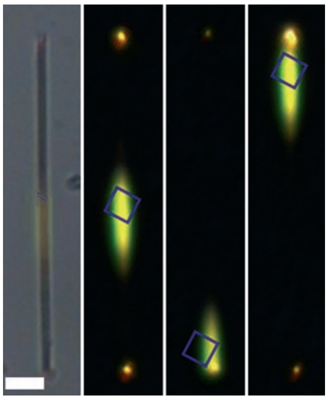

Light at the end of the tunnel: Two kinds of 1D microstructures, tubes and rods, were prepared from 9,10-bis(phenylethynyl)anthracene. While both types of 1D microstructures can absorb excitation light and propagate the photoluminescence (PL) emission towards the tips, the air inside the hollow tubes changes the waveguide behavior and helps to reduce the optical loss (see PL images, scale bar: 10 µm).

Copolymerization

S. S, J. K. Min, J. E. Seong, S. J. Na,
B. Y. Lee* ______ **7306 – 7309**

A Highly Active and Recyclable Catalytic System for CO_2/Propylene Oxide Copolymerization

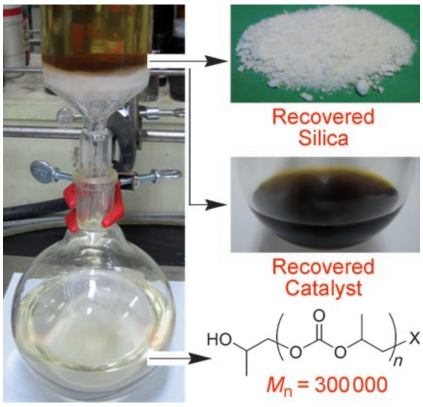

Converting CO_2 into polymer: A catalytic system that produces a high molecular weight CO_2/propylene oxide copolymer with high activity and selectivity is disclosed. After filtration through silica gel, elution of the catalyst leaves a solid phase with a negligible metal residue (see picture). The catalyst can be reused without significant loss of performance.

VIP Natural Products

K. C. Nicolaou,* Y.-P. Sun, X.-S. Peng,
D. Polet, D. Y.-K. Chen* ______ **7310 – 7313**

Total Synthesis of (+)-Cortistatin A

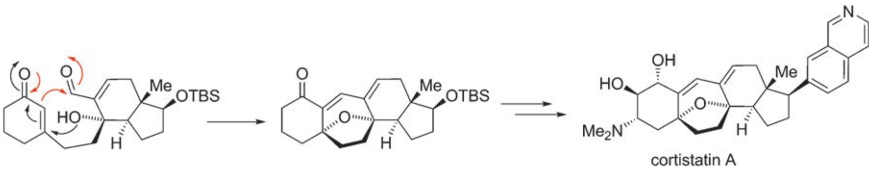

Marine engineering: A modular strategy featuring an intramolecular 1,4-addition/aldol/dehydration cascade sequence (see scheme; TBS = *tert*-butyldimethylsilyl) has enabled the total synthesis of cortistatin A, a potent anti-angiogenic marine natural product. This flexible route offers access to other members of the cortistatin family, both natural and designed.

Natural Product Synthesis

T. J. Donohoe,* A. Ironmonger,
N. M. Kershaw ______ 7314 – 7316

Synthesis of (−)-(*Z*)-Deoxypukalide

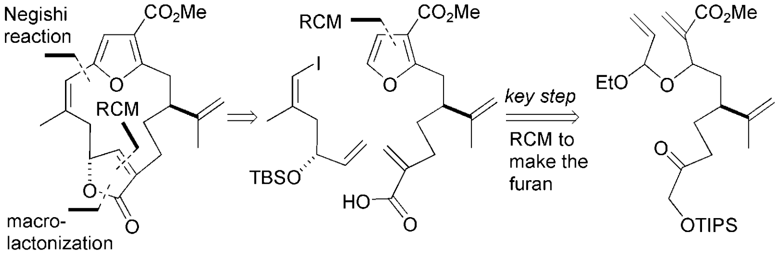

(−)-(*Z*)-deoxypukalide

Closing the deal: A ring-closing metathesis (RCM)/aromatization protocol, followed by a regioselective Negishi cross-coupling reaction and macrolactonization, with subsequent RCM mediate the synthesis of (−)-(*Z*)-deoxypukalide in 12 linear steps and 15 % overall yield (see retrosynthesis; TBS = *tert*-butyldimethylsilyl, TIPS = triisopropylsilyl).

Natural Product Synthesis

M. E. Green, J. C. Rech,
P. E. Floreancig* ______ 7317 – 7320

Total Synthesis of Theopederin D

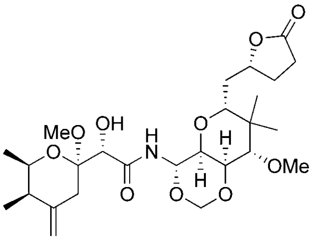

theopederin D

The transformation is complete! The total synthesis of theopederin D (see structure), a potent cytotoxin, has been achieved through oxidative cleavage of a carbon–carbon bond. Other key transformations include an acid-mediated functionalization of a tetrahydrofuranol, a *syn*-selective glycal epoxide ring-opening, and an asymmetric aldehyde/acid chloride condensation.

Enzyme Models

Y. J. Jeong, Y. Kang, A.-R. Han, Y.-M. Lee,
H. Kotani, S. Fukuzumi,*
W. Nam* ______ 7321 – 7324

Hydrogen Atom Abstraction and Hydride Transfer Reactions by Iron(IV)–Oxo Porphyrins

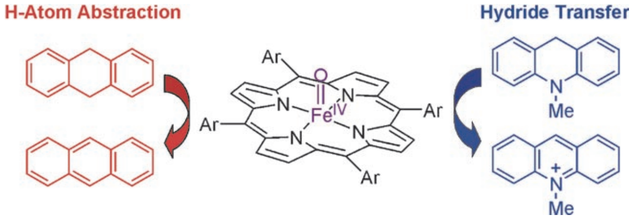

True identity revealed: The C−H bond activation of alkyl aromatics by synthetic iron(IV)–oxo porphyrin species and the hydride transfer of NADH analogues to them occur through H-atom abstraction and proton-coupled electron-transfer mechanisms, respectively. Mechanistic studies revealed that iron(IV)–oxo porphyrins, not iron(IV)–oxo porphyrin π-radical cations, are the true oxidant.

Oxidation

T.-C. Kao, G. J. Chuang,
C.-C. Liao* ______ 7325 – 7327

Photooxygenation of Masked *o*-Benzoquinones: An Efficient Entry into Highly Functionalized Cyclopentenones from 2-Methoxyphenols

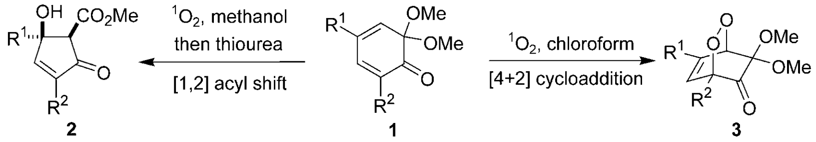

MOB tactics: A novel oxidation of masked *o*-benzoquinones (MOBs) **1** occurs by singlet-oxygen-triggered ring contraction to form cyclopentenone derivatives **2** and by [4+2] cycloaddition to give endoperoxides **3**. The competing pathways are directed by solvents and allow access to a variety of functionalized cyclopentenes.

Solid-State NMR Spectroscopy

D. H. Zhou, C. M. Rienstra* **7328 – 7331**

Rapid Analysis of Organic Compounds by Proton-Detected Heteronuclear Correlation NMR Spectroscopy with 40 kHz Magic-Angle Spinning

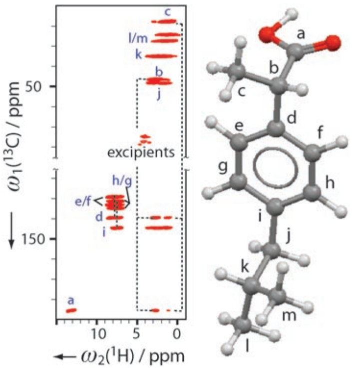

High-sensitivity proton detection enabled acquisition of well-resolved two-dimensional spectra in only 30 minutes for less than 5 mg of organic compounds at natural abundance. Besides faster resonance assignment, rapid analysis of crystal polymorphism, molecular dynamics, and H-bonding is possible. This method is applicable to both pure and dosage forms of solid pharmaceuticals, such as ibuprofen (see picture).

Cell Imaging

H. V. K. Diyabalanage, K. Ganguly,
D. S. Ehler, G. E. Collis, B. L. Scott,
A. Chaudhary, A. K. Burrell,
T. M. McCleskey* **7332 – 7334**

Three-Coordinate Ligand for Physiological Beryllium Imaging by Fluoresence

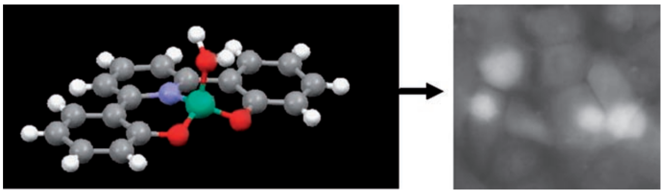

To Be or not to Be: Be binds strongly to the three-dentate ligand 2,6-bis(2-hydroxyphenyl)pyridine in a 1:1 ratio with no bridging phenolates (see structure; Be green, C gray, H white, O red, N blue). As Be binds and displaces the strong hydrogen bonds, the ligand fluoresces. The fluorescence is very specific for Be and can be used to detect beryllium in cells, as demonstrated with human lung epithelial cells (see picture, right).

Water Oxidation

R. Brimblecombe, G. F. Swiegers,*
G. C. Dismukes,*
L. Spiccia* **7335 – 7338**

Sustained Water Oxidation Photocatalysis by a Bioinspired Manganese Cluster

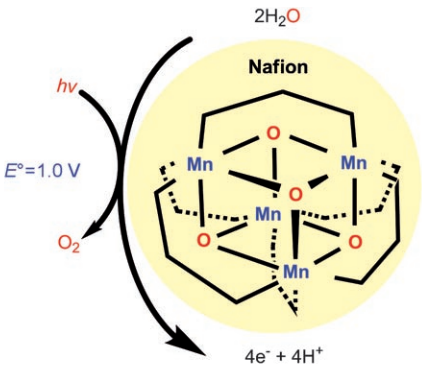

The generation game: A manganese–oxo complex with a cubic $\{Mn_4O_4\}^{7+}$ core catalyzes the electrooxidation of water when suspended within the aqueous channels of a Nafion membrane (see picture). Illumination with visible light under an applied potential of 1.0 V (vs Ag/AgCl) generates current over one thousand turnovers. The catalytically active species arises from photolysis and subsequent dissociation of the manganese complex.

Asymmetric Catalysis

D. Chen, M. Schmitkamp, G. Franciò,
J. Klankermayer,*
W. Leitner* **7339 – 7341**

Enantioselective Hydrogenation with Racemic and Enantiopure Binap in the Presence of a Chiral Ionic Liquid

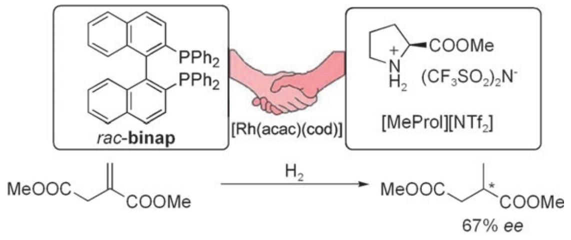

Racemic but enantioselective: *rac*-Binap and a chiral ionic liquid (cIL) used for the asymmetric hydrogenation of dimethyl itaconate led to identical *ee* values as enantiopure binap. The enantiodifferentiation results primarily from a diastereomeric interaction of the binap–Rh unit and the proline ester moiety. For other substrates, enhanced enantioselectivity with inverted absolute configuration was obtained with the enantiopure ligand in the cIL relative to organic solvents.

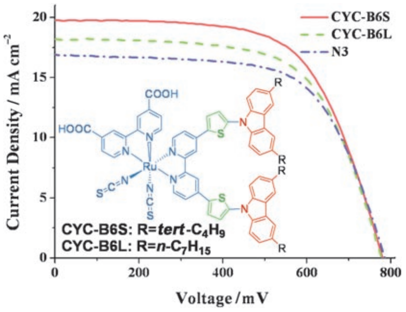

The sensitive type: Two new ruthenium-based supersensitizers (CYC-B6S and CYC-B6L) in which a hole-transport moiety and a conjugated segment are connected sequentially to the bipyridine of the ancillary ligand show efficiency in dye-sensitized solar cells (DSCs) of up to 9.72%. Increasing the conversion efficiency of liquid-state DSCs by connecting a carbazole moiety to the ancillary ligand of the ruthenium-based sensitizer is demonstrated.

Dye-Sensitized Solar Cells

C.-Y. Chen, J.-G. Chen, S.-J. Wu, J.-Y. Li, C.-G. Wu,* K.-C. Ho* ______ **7342 – 7345**

Multifunctionalized Ruthenium-Based Supersensitizers for Highly Efficient Dye-Sensitized Solar Cells

---

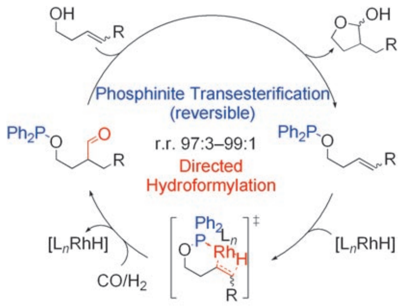

Phosphinites do the trick and work as reversibly bound catalyst-directing groups in catalytic amounts to allow for the highly regioselective hydroformylation of homoallylic alcohols with terminal and internal alkene functions in favor of the branched product.

Homogeneous Catalysis

C. U. Grünanger, B. Breit* _ **7346 – 7349**

Branched-Regioselective Hydroformylation with Catalytic Amounts of a Reversibly Bound Directing Group

---

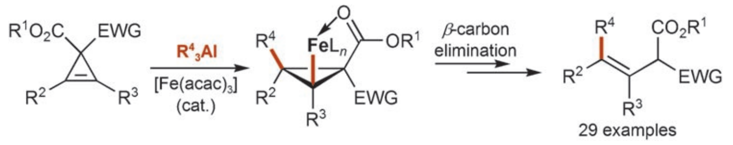

Open sesame: An iron-catalyzed cyclopropene carbometalation ring-opening sequence using trialkylaluminum reagents is described. The reactions proceed with high levels of regio- and stereocontrol to provide a range of multisubstituted alkenes, including trisubstituted vinylsilanes, trisubstituted vinylstannanes, and all-carbon tetrasubstituted alkenes.

Alkene Synthesis

Y. Wang, E. A. F. Fordyce, F. Y. Chen, H. W. Lam* ______ **7350 – 7353**

Stereoselective Synthesis of Tri- and Tetrasubstituted Alkenes by Iron-Catalyzed Carbometalation Ring-Opening Reactions of Cyclopropenes

---

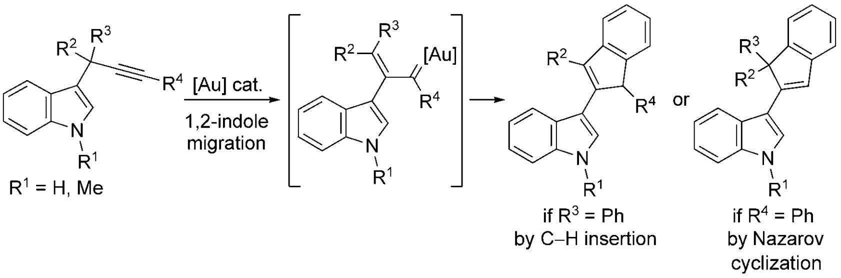

Take your pick! Indene-containing indole scaffolds have been catalytically prepared from C3-propargylated indoles by tandem reactions involving an initial 1,2-indole migration. This unprecedented process generates a gold carbene complex and proceeds through either a formal C–H insertion or a Nazarov cyclization (see scheme).

Gold Catalysis

R. Sanz,* D. Miguel, F. Rodríguez ______ **7354 – 7357**

Gold(I)-Catalyzed Tandem Reactions Initiated by 1,2-Indole Migrations

Asymmetric Conjugate Additions

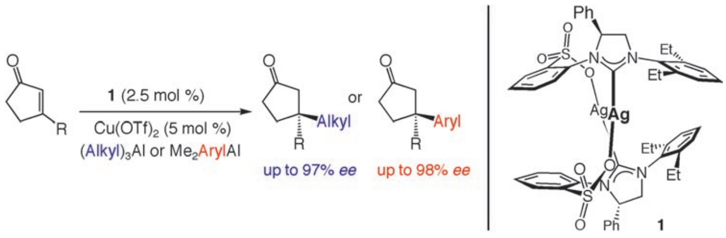

Solution to pesky problems: Effective methods for catalytic asymmetric conjugate additions of alkyl and aryl aluminum reagents with unactivated β-substituted cyclopentenones are now available (see scheme). Transformations, promoted by chiral bidentate N-heterocyclic carbene (NHC) copper complexes derived from **1**, give rise to all-carbon quaternary stereogenic centers.

Supporting information is available on www.angewandte.org (see article for access details).

A video clip is available as Supporting Information on www.angewandte.org (see article for access details).

Service